Electronic Supplementary Material (ESI) for ChemComm.

SUPPORTING INFORMATION

Improved Synthesis Enable Assessment of the Electrochemical Window of Monocarborate Solid State Electrolytes

Oscar Tutusaus[1], Hiroko Kuwata[1], Michael J. Counihan[1], Rana Mohtadi[1,2a]

1)Toyota Research Institute of North America, 1555 Woodridge Avenue, Ann Arbor, MI 48105, USA

2) Advanced Institute for Materials Research (AIMR), Tohoku University, Katahira 2-1-1, Aoba-ku, Sendai, 980-8577, Japan

[a] Author to whom correspondence should be addressed: rana.mohtadi@toyota.com

Materials and methods: All water-free synthesis and handling of moisture-sensitive salts were performed in an argon-filled MBraun glovebox maintained below 0.1 ppm of O_2 and H_2O. $CsCB_9H_{10}$, $CsCB_{11}H_{12}$, $HNEt_3CB_{11}H_{12}$ and $HNEt_3CB_9H_{10}$ were obtained from Katchem and used as received. All other materials were obtained from Sigma-Aldrich. LiHMDS was recrystallized from hexane prior to use. Tetrahydrofuran and hexane were purchased in anhydrous form and further dried by storage over 3 Å molecular sieves for a minimum of 24 hours prior to use.

Characterization: NMR spectra were obtained on a Varian Vnmrs700 instrument in DMSO-d_6. Raman spectroscopy was performed under argon on a Horiba LabRAM HR Microspectrometer using a 532 nm excitation laser. The XRD measurements were conducted in Rigaku SmartLab® equipped with Cu Kα Xray source. To prevent exposure to air, the material was loaded in quartz capillaries and measured at 0.05° step size between 5-80°.

Electrochemical testing: For metal plating and striping tests, the electrolyte material was uniaxially pressed at 486 MPa to obtain a pellet of 11 mm diameter and 0.5 mm thickness. This pellet was sandwiched between a surface-scratched Li or Na metal disk (11 mm diameter) and a stainless steel disk (11 mm diameter, 0.012 mm thickness). Stainless steel disks were prepared from foil that was first polished with 0.3 µm Al_2O_3 micropolish suspension (Buehler) and rinsed with water, then punched into 11 mm diameter disks, which were first sonicated with acetone/water (1:1) and then with water, and finally dried in a vacuum oven at 80 °C. The sandwiched pellet was assembled in a cell between two stainless steel rods with a constant torque of 0.3 Nm.

For oxidative stability evaluation, pellets of 11 mm diameter consisting of an electrolyte composite layer (0.3 mm thickness) and an electrolyte layer (0.5 mm thickness) were prepared by uniaxially pressing the electrolyte material under 81 MPa, followed by adding a powder stack of electrolyte composite prepared as described below and uniaxially pressing again at 486 MPa. A stainless steel disk (11 mm diameter, 0.012 mm) prepared as explained above was attached to the electrolyte composite side of the pellet and a surface-scratched Li or Na metal disk (11 mm diameter) was attached to the electrolyte layer side of the pellet. All components were assembled in a cell between two stainless steel rods with a constant torque of 3.5 Nm. Electrolyte composites used above were prepared by mixing the electrolyte material and stainless steel powder in a volume ratio 1:1 with agate mortar and pestle for 5 minutes. We selected stainless steel over carbon as conductive material to avoid any potential parasitic effects resulting from interaction between carbon surface groups and electrolyte material. The oxidative stability was measured on a planar stainless steel electrode (11 mm diameter, 0.012 mm) prepared as described above. For the DC polarization measurements, the working electrode was the electrolyte-stainless steel composite described before, that was attached to a stainless steel planar electrode (11 mm diameter, 0.012 mm). In these experiments, the voltage was set to a predetermined value that was held for 3 hours then progressively increased. The current response at each of these voltages was recorded. The cycling performances of metal plating and stripping were evaluated by CV between -0.5 V and 3.050 V (vs. Li/Li^+) and -0.5 V and 2.8 V (vs. Na/Na^+) at room temperature and 0.1 mV/s scan rate. Electrochemical oxidative stability was assessed by CV between 2.0 V and 5.8 V at room temperature and 0.1 mV/s scan rate.

Oxidative stability was determined from the intersection of two straight lines obtained by linear regression of (i) the nonfaradaic current associated with the double layer capacitance and (ii) the faradaic anodic current. Two cells were tested for each of the electrolytes. For the conductivity measurements, the solid state electrolyte was grinded using a mortar and pestle then uniaxially pressing it at 486 MPa pressure for 10 min, sandwiched between carbon coated aluminium foils (11 mm diameter, 0.02 mm thickness). The cell then was torqued at 3.5 N.m and allowed to equilibrate for about 4 hours at 30 °C before the impedance measurement was taken. All electrochemical measurements were performed on a Biologic VMP3 multi-channel potentiostat.

$LiCB_{11}H_{12}$ (aqueous route). A solution of $CsCB_{11}H_{12}$ (10 g, 36.2 mmol) in H_2O (60 mL) at 50 °C was passaged through a column of cation exchange resin (Dowex 50W-X8, Li^+ form, 135 mL). The aqueous solution containing $LiCB_{11}H_{12}$ was evaporated to dryness and the resulting solid was further dried under vacuum at 120 °C for 16 h and at 160 °C for 24 h. Yield: 5.27 g (97%). Residual H_2O (^{1}H NMR): 522 ppm.

$LiCB_{11}H_{12}$ (water-free route). A solution of LiHMDS (7.9 g, 47.2 mmol) in dry THF (25 mL) was added in 5 mL portions to a stirring solution of $HNEt_3CB_{11}H_{12}$ (11 g, 44.9 mmol) in dry THF (115 mL) cooled at 10 °C. The suspension was heated until all solid dissolved (35 °C). Dry hexane (100 mL) was added and the resulting suspension was cooled to 10 °C while stirring for 1 hour. The solid was collected by filtration, washed with dry THF/hexane (7:5, 24 mL) and dry hexane (2x40 mL), then transferred to a crystallization dish and heated under argon flow to 160 °C for 1.5 h and 250 °C for 48 h. Yield: 6.39 g (95%).

$LiCB_9H_{10}$ (water-free route). A solution of LiHMDS (9.52 g, 56.9 mmol) in dry THF (25 mL) was added in 5 mL portions to a stirring solution of $HNEt_3CB_9H_{10}$ (12 g, 54.2 mmol) in dry THF (45 mL) cooled at 10 °C. The suspension was heated until all solid dissolved (23 °C). Dry hexane (140 mL) was added and the resulting suspension was cooled to 10 °C while stirring for 1 hour. The solid was collected by filtration, washed with dry THF/hexane (1:2, 24 mL) and dry hexane (2x40 mL), then transferred to a crystallization dish and heated under argon flow to 140 °C for 1 h, 200 °C for 1 h and 250 °C for 48 h. Yield: 6.76 g (99%).

$NaCB_{11}H_{12}$. A solution of $CsCB_{11}H_{12}$ (3.32 g, 12 mmol) in H_2O (60 mL) at 50 °C was passaged through a column of cation exchange resin (Dowex 50W-X8, Na^+ form, 75 mL). The aqueous solution containing $NaCB_{11}H_{12}$ was evaporated to dryness and the resulting solid was further dried at 100 °C for 16 h under vacuum and at 200 °C for 24 h under argon flow. Yield: 1.92 g (96%). Residual H_2O (^{1}H NMR): 94 ppm.

$NaCB_9H_{10}$. A solution of $CsCB_9H_{10}$ (1.89 g, 7.5 mmol) in H_2O (60 mL) at 50 °C was passaged through a column of cation exchange resin (Dowex 50W-X8, Na^+ form, 27 mL). The aqueous solution containing $NaCB_9H_{10}$ was evaporated to dryness and the resulting solid was further dried under vacuum at 100 °C for 16 hours and 160 °C for 16 h. Yield: 1.02 g (96%). Residual H_2O (^{1}H NMR): 29 ppm.

Table S1. Summary of reported methods for the synthesis of unsolvated Na or Li salts of $CB_{11}H_{12}$ or/and CB_9H_{10} anions, sorted chronologically.

Solvated salt origin	Drying method	Ref
Ion exchange of $[Et_3NH]CB_{11}H_{12}$ to $[H_3O]CB_{11}H_{12}$, followed by neutralization with 0.1M XOH (X=Na or Li) until pH=7 and water evaporation.	Under vacuum at 160 °C ($LiCB_{11}H_{12}$) and 57 °C ($NaCB_{11}H_{12}$).	1
$LiCB_{11}H_{12}$ and $NaCB_{11}H_{12}$ were obtained commercially.	Under vacuum at 160 °C ($LiCB_{11}H_{12}$) and 80 °C ($NaCB_{11}H_{12}$) for 6 h.	2
$LiCB_9H_{10}{\cdot}xH_2O$, $NaCB_9H_{10}$, $LiCB_{11}H_{12}{\cdot}xH_2O$, and $NaCB_{11}H_{12}$ were obtained commercially. $Li_2(CB_9H_{10})(CB_{11}H_{12})$ and $Na_2(CB_9H_{10})(CB_{11}H_{12})$ were synthesized by first dissolving equimolar amounts of the respective pure anhydrous components in water followed by solid-hydrate precipitation by room-temperature evacuation of the excess water.	Under vacuum at 200 °C, 160 °C, 160 °C and 80 °C overnight, respectively. Under vacuum at 200 °C overnight.	3
$LiCB_9H_{10}{\cdot}xH_2O$ and $NaCB_9H_{10}$ were obtained commercially.	"Hours of evacuation" between 160 °C and 200 °C.	4
Acid-base reaction of an aqueous solution of $(NMe_3H)CB_{11}H_{12}$ with excess LiOH, then evaporation to dryness. The solid was added H_2O and extracted with Et_2O; organic phase was washed with an aqueous solution of LiOH (10%), LiCl (20%), and water, then dried first with powdered activated molecular sieves and then with LiH, followed by solvent evaporation. The obtained oil was dissolved in CH_3CN, stirred with activated charcoal, followed by solvent removal.	Acetonitrile solvate was dried under reduced pressure (10 Pa) at 130 °C for 7 days.	5
Deprotonation of $(NMe_3H)CB_{11}H_{12}$ with excess LiH in CH_3CN; excess LiH removed by filtration, followed by solvent removal.	Acetonitrile solvate was dried under reduced pressure (10 Pa) at 130 °C for 7 days.	6
$NaCB_{11}H_{12}$ was obtained commercially.	Under dynamic vacuum at 250 °C for 12 h.	7
$NaCB_9H_{10}$ and $NaCB_{11}H_{12}$ were obtained commercially.	Under vacuum ($<10^{-3}$ mbar) at 160 °C for 6 h.	8
[Hydrated] $LiCB_9H_{10}$ and $LiCB_{11}H_{12}$ were obtained commercially. $Li_2(CB_9H_{10})(CB_{11}H_{12})$ was prepared using an equimolar mixture of pre-dried $LiCB_9H_{10}$ and $LiCB_{11}H_{12}$ after dissolution in anhydrous isopropanol and rotary evaporation.	Under vacuum at 200 °C ($LiCB_9H_{10}$) and 160 °C ($LiCB_{11}H_{12}$) for 12 h. Under vacuum at 150 °C for 1 h, then heat-treated under vacuum at 200 °C for 4 h.	9

$LiCB_9H_{10}{\cdot}xH_2O$ and $LiCB_{11}H_{12}{\cdot}xH_2O$ were obtained commercially.	Under vacuum (<5 × 10^{-4} Pa) at 200 °C for 12 h ($LiCB_9H_{10}$) and 160 °C for 12 h ($LiCB_{11}H_{12}$).	10
$NaCB_{11}H_{12}$ was obtained commercially.	Under vacuum (10^{-3} mbar) at 250 °C for 12 h.	11
$LiCB_9H_{10}$, $LiCB_{11}H_{12}$, $NaCB_9H_{10}$ and $NaCB_{11}H_{12}$ were obtained commercially.	Under dynamic vacuum (≈10^{-3} mbar) at 200 °C overnight (at least 12 h).	12
$LiCB_9H_{10}(H_2O)$ and $LiCB_{11}H_{12}(H_2O)_{0.5}$ were obtained commercially.	At 180°C for 12 h.	13
$NaCB_9H_{10}{\cdot}xH_2O$ and $NaCB_{11}H_{12}{\cdot}xH_2O$ were obtained commercially.	Under vacuum at 120 °C overnight.	14
$NaCB_{11}H_{12}$ was obtained commercially.	Under dynamic vacuum (≈10^{-3} mbar) at 180 °C for 12 h .	15

(1) W. S. Tang, A. Unemoto, W. Zhou, V. Stavila, M. Matsuo, H. Wu, S.-i. Orimo and T. J. Udovic, *Energy Environ. Sci.*, 2015, **8**, 3637.
(2) A. V. Skripov, R. V. Skoryunov, A. V. Soloninin, O. A. Babanova, W. S. Tang, V. Stavila and T. J. Udovic, *J. Phys. Chem. C*, 2015, **119**, 26912.
(3) W. S. Tang, K. Yoshida, A. V. Soloninin, R. V. Skoryunov, O. A. Babanova, A. V. Skripov, M. Dimitrievska, V. Stavila, S.-i. Orimo and T. J. Udovic, *ACS Energy Lett.*, 2016, **1**, 659.
(4) W. S. Tang, M. Matsuo, H. Wu, V. Stavila, W. Zhou, A. A. Talin, A. V. Soloninin, R. V. Skoryunov, O. A. Babanova, A. V. Skripov, A. Unemoto, S.-i. Orimo and T. J. Udovic, *Adv. Energy Mat.*, **6**, 1502237.
(5) Y. Kitazawa, R. Takita, K. Yoshida, A. Muranaka, S. Matsubara and M. Uchiyama, *J. Org. Chem.*, 2017, **82**, 1931.
(6) J. F. Kleinsasser, S. P. Fisher, F. S. Tham and V. Lavallo, *Eur. J. Inorg. Chem.*, 2017, **38-39**, 4417.
(7) M. Brighi, F. Murgia, Z. Łodziana, P. Schouwink, A. Wołczyk and R. Černý, *J. Power Sources*, 2018, **404**, 7.
(8) L. Duchêne, S. Lunghammer, T. Burankova, W.-C. Liao, J. P. Embs, C. Copéret, H. M. R. Wilkening, A. Remhof, H. Hagemann and C. Battaglia, *Chem. Mater.*, 2019, **31**, 3449.
(9) R. Asakura, L. Duchêne, R.-S. Kühnel, A. Remhof, H. Hagemann and C. Battaglia, *ACS Appl. Energy Mater.*, 2019, **2**, 6924.
(10) (a) S. Kim, H. Oguchi, N. Toyama, T. Sato, S. Takagi, T. Otomo, D. Arunkumar, N. Kuwata, J. Kawamura anb S.-i. Orimo, *Nat. Commun.*, 2019, **10**, 1081; (b) S. Kim, K. Kisu, S. Takagi, H. Oguchi and S.-i. Orimo, *ACS Appl. Energy Mater.*, 2020, **3**, 4831.
(11) R. Asakura, D. Reber, L. Duchêne, S. Payandeh, A. Remhof, H. Hagemann and C. Battaglia, *Energy Environ. Sci.*, 2020, **13**, 5048.
(12) M. Brighi, F. Murgia and R. Černý, *Cell Rep. Phys. Sci.*, 2020, **1**, 100217.
(13) S. Payandeh, D, Rentsch, Z. Łodziana, R. Asakura, L. Bigler, R. Černý, C. Battaglia and A. Remhof, *Adv. Funct. Mater.* 2021, 2010046
(14) K. Niitani, S. Ushiroda, H. Kuwata, H. N. Ohata, Y. Shimo, M. Hozumi, T. Matsunaga and S. Nakanishi, *ACS Energy Lett.*, 2022, **7**, 145.
(15) M. Brighi, F. Murgia and R. Černý, *Adv. Mater. Interfaces*, 2022, **9**, 2101254.

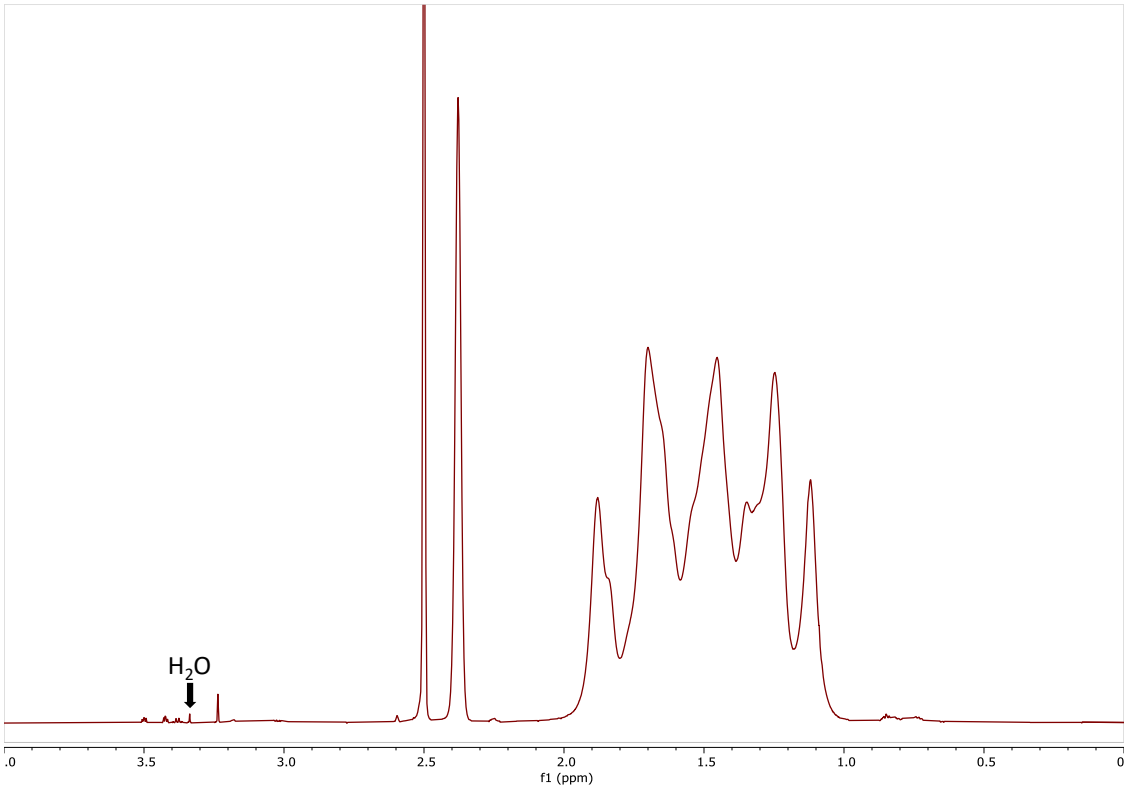

Figure S1. ^{1}H NMR spectrum of $NaCB_{11}H_{12}$ in DMSO-d_6.

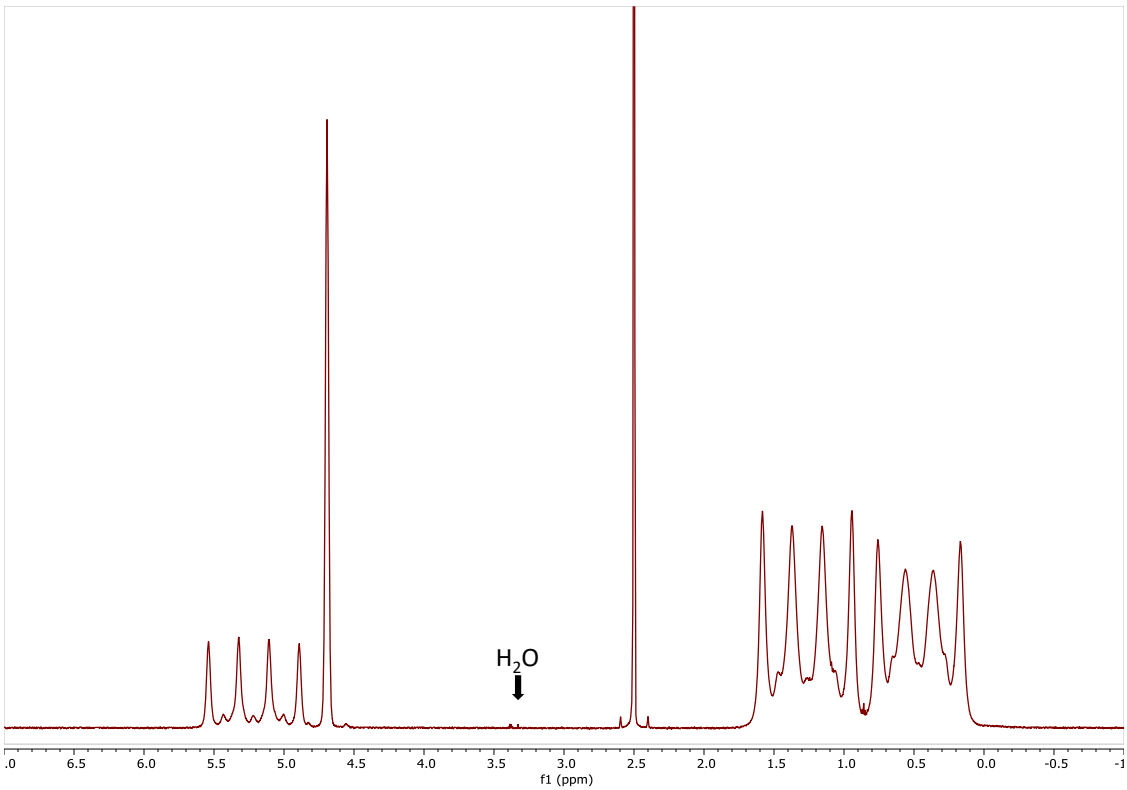

Figure S2. ^{11}H NMR spectrum of $NaCB_9H_{10}$ in DMSO-d_6.

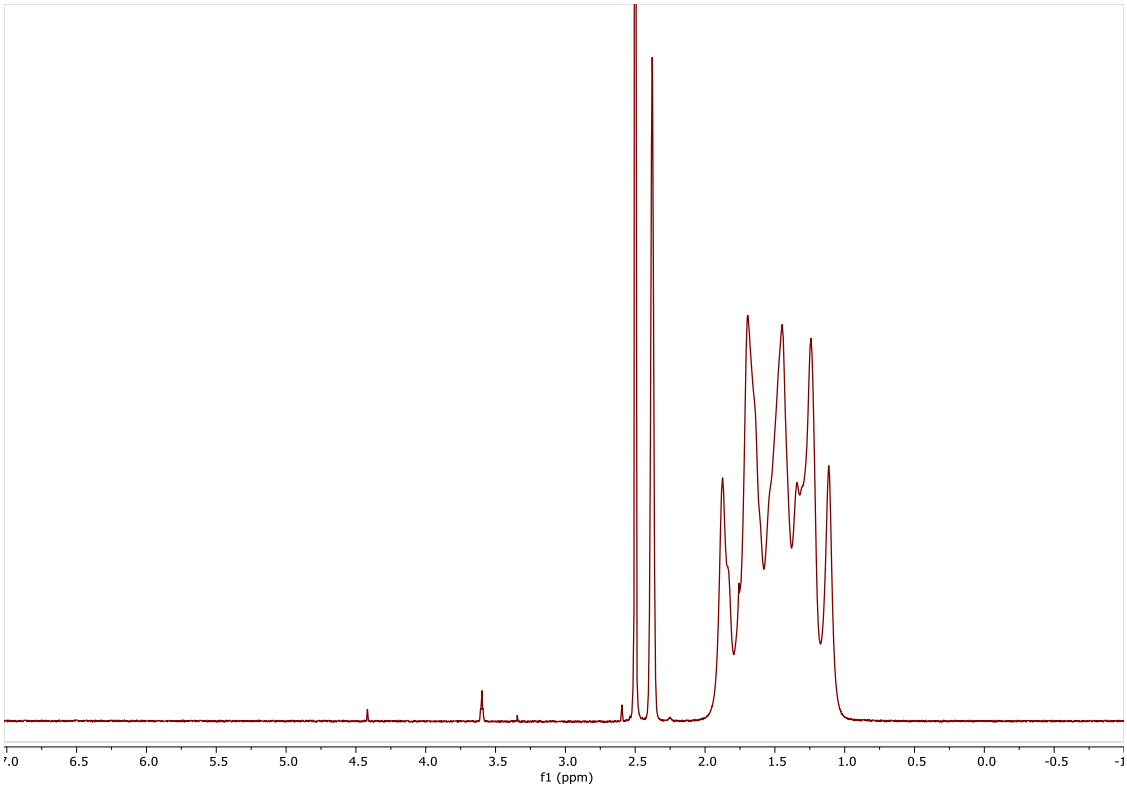

Figure S3. ^{1}H NMR spectrum of $LiCB_{11}H_{12}$ (prepared using non-aqueous route) in DMSO-d_6.

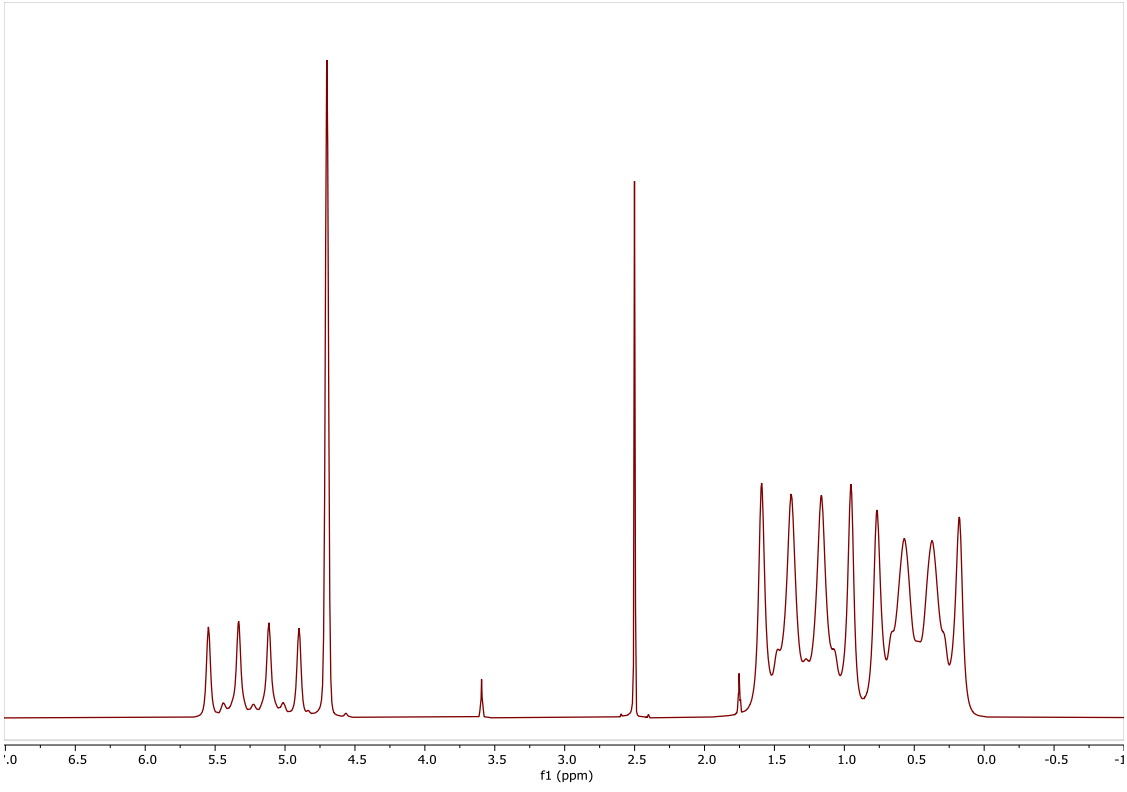

Figure S4. ^{1}H NMR spectrum of $LiCB_9H_{10}$ (prepared using non-aqueous route) in DMSO-d_6.

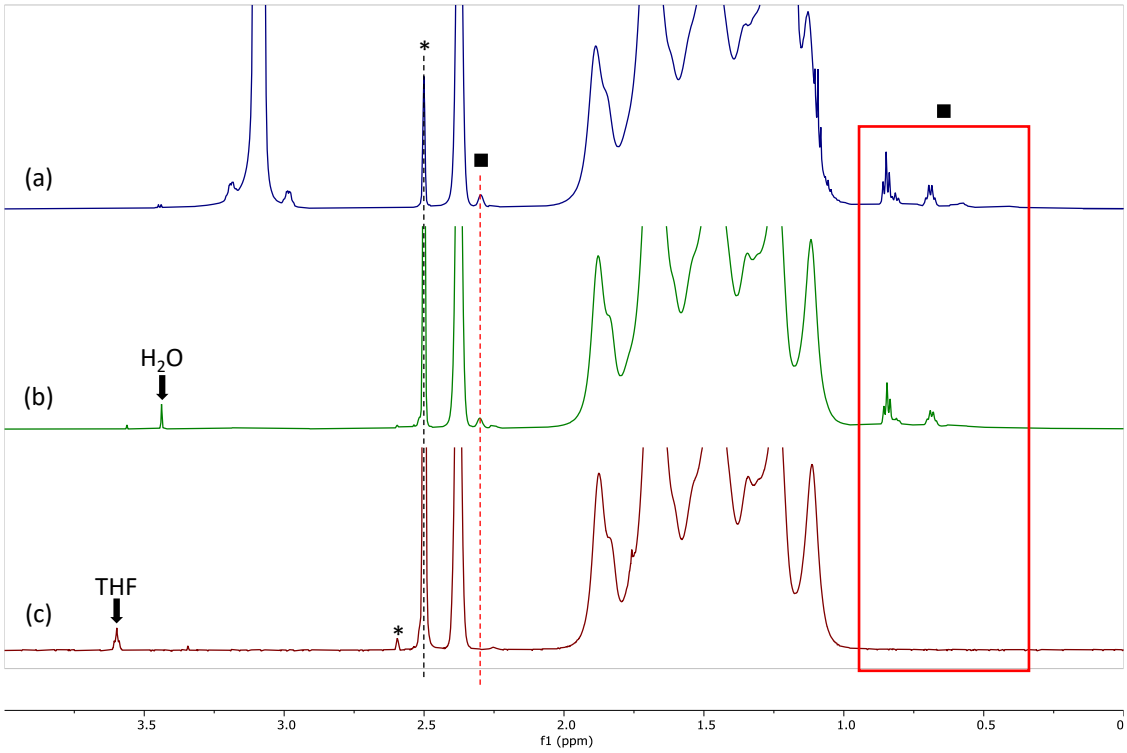

Figure S5. ^{1}H NMR spectra of (a) $HNEt_3CB_{11}H_{12}$, (b) $LiCB_{11}H_{12}$ obtained via aqueous route, (c) $LiCB_{11}H_{12}$ obtained via water-free route. * DMSO, ■ Impurities

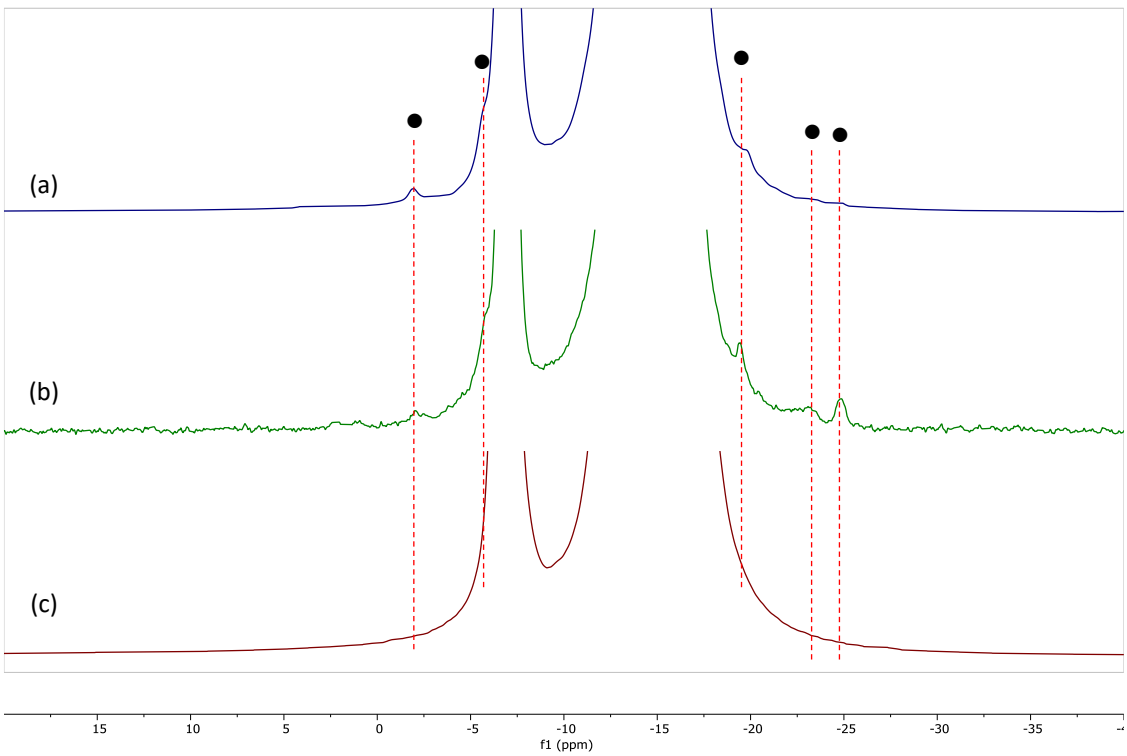

Figure S6. $^{11}B\{^{1}H\}$ NMR spectra of (a) $HNEt_3CB_{11}H_{12}$, (b) $LiCB_{11}H_{12}$ obtained via aqueous route, (c) $LiCB_{11}H_{12}$ obtained via water-free route. ● Impurities

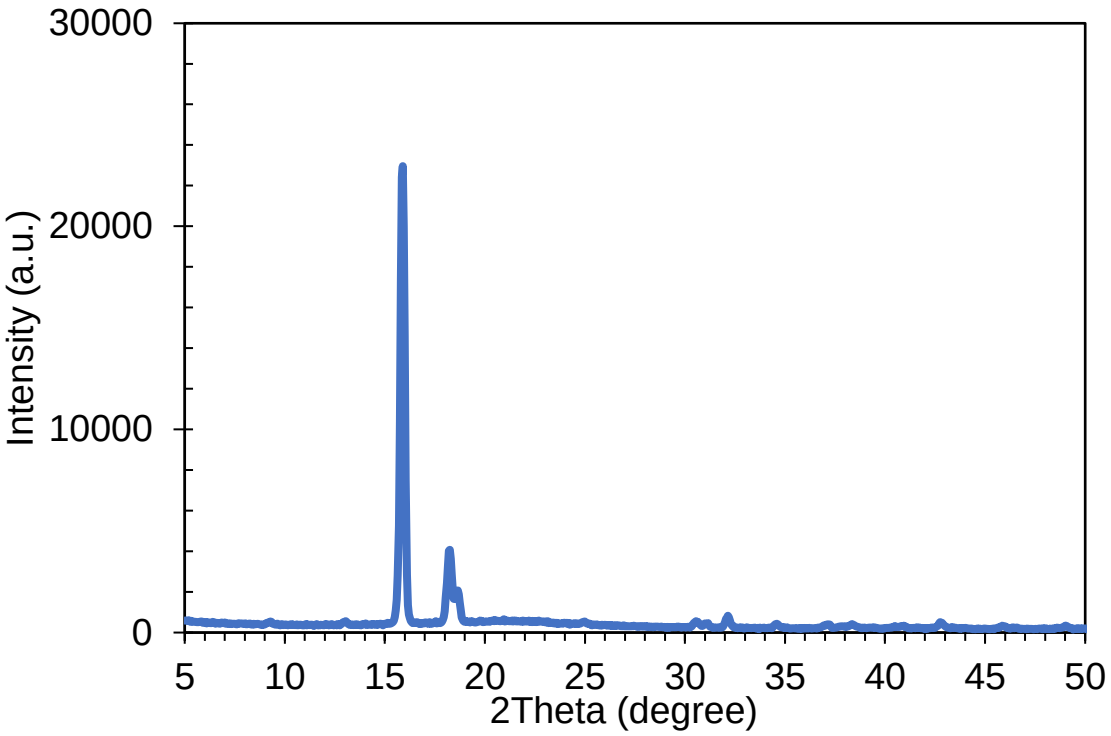

Figure S7. XRD results of $LiCB_{11}H_{12}$ produced through the anhydrous synthesis process.

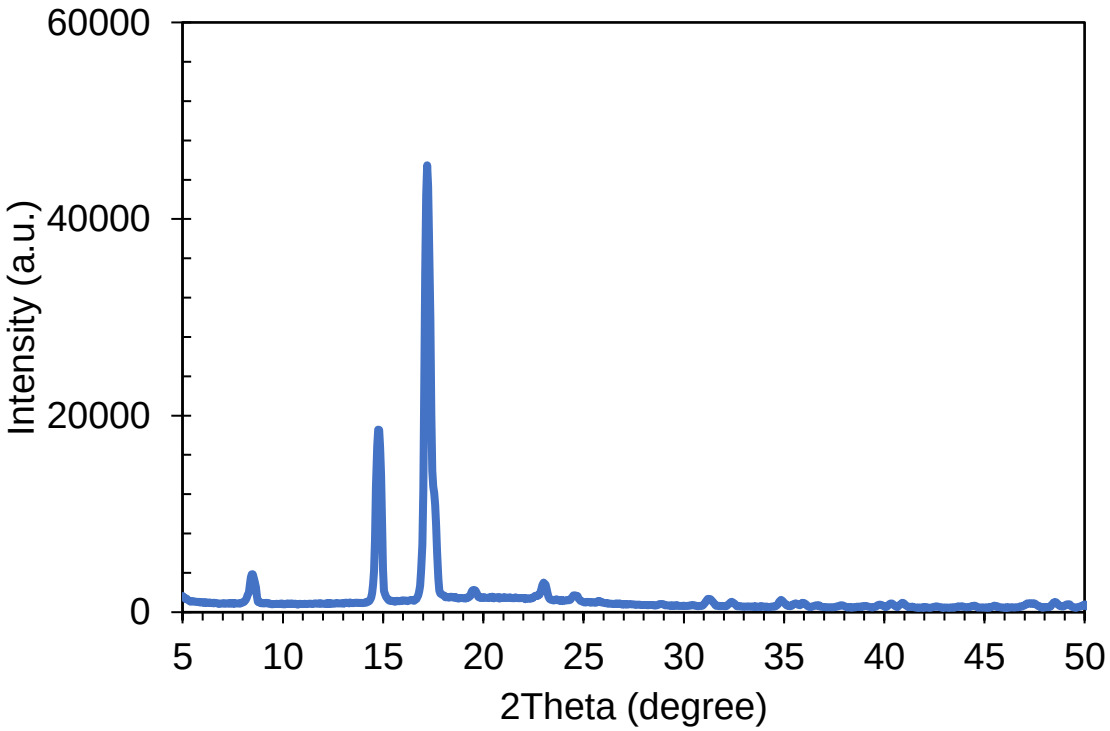

Figure S8. XRD results of $LiCB_9H_{10}$ produced through the anhydrous synthesis process.

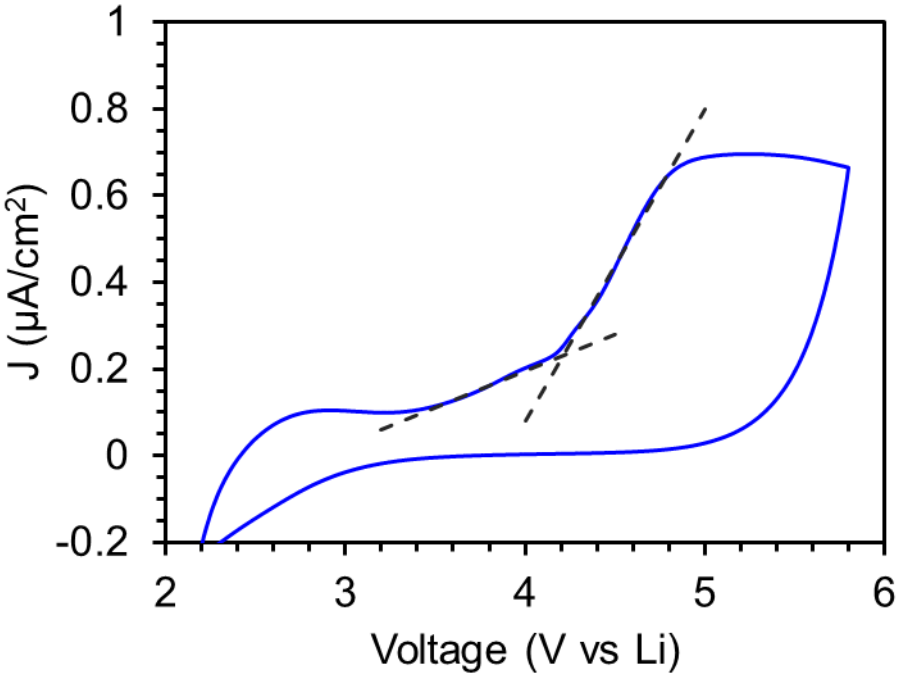

Figure S9. Cyclic voltammetry curve of $LiCB_{11}H_{12}$ in Li/SE/SE-SS/SS (SS=stainless steel) at a scan rate of 0.1 mV/s at 25°C.

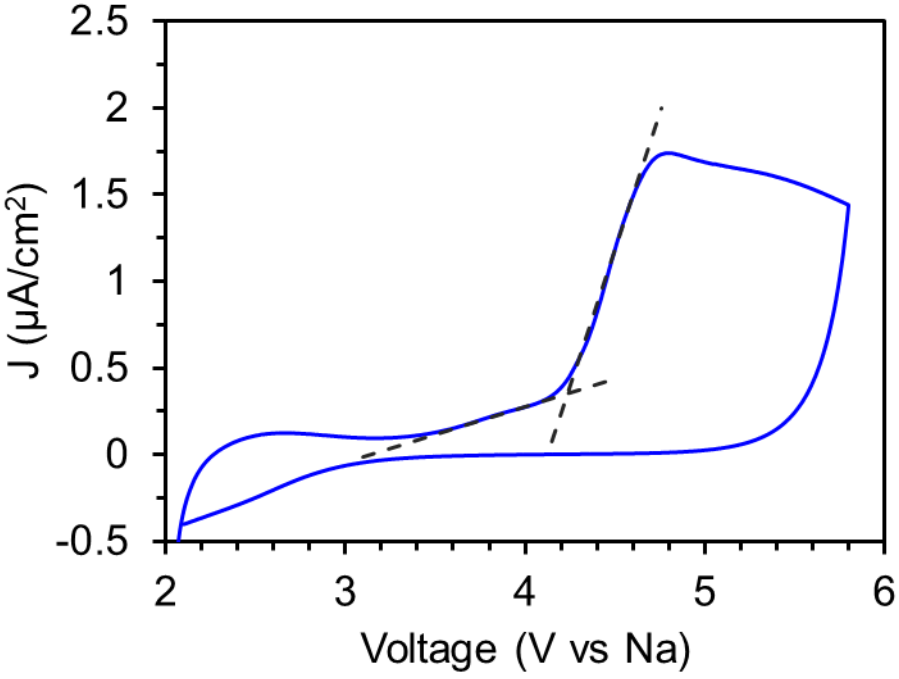

Figure S10. Cyclic voltammetry curve of $NaCB_{11}H_{12}$ in Na/SE/SE-SS/SS (SS=stainless steel) at a scan rate of 0.1 mV/s at 25°C.

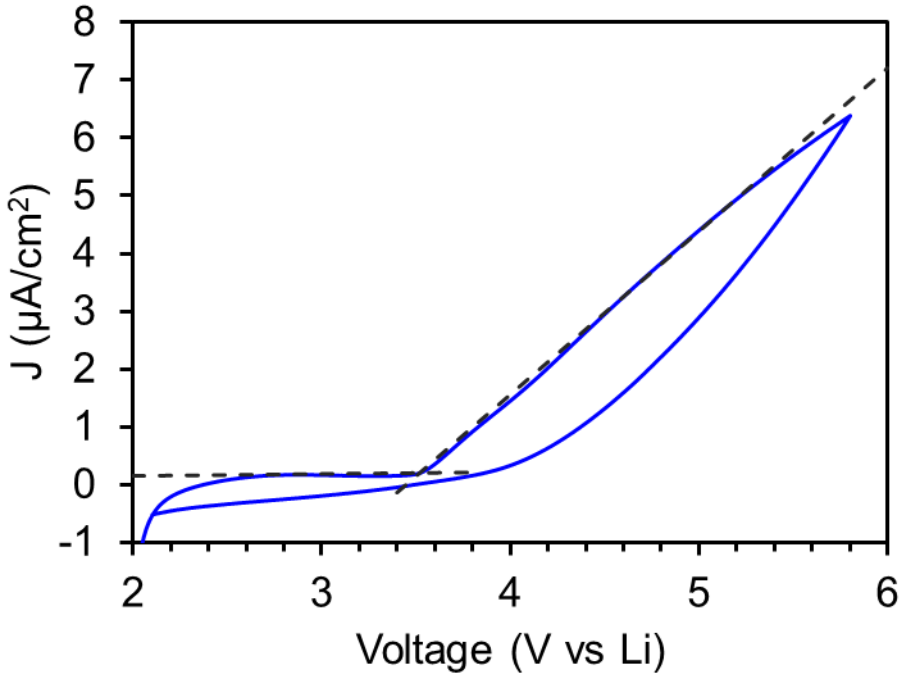

Figure S11. Cyclic voltammetry curve of $LiCB_9H_{10}$ in Li/SE/SE-SS/SS (SS=stainless steel) at a scan rate of 0.1 mV/s at 25°C.

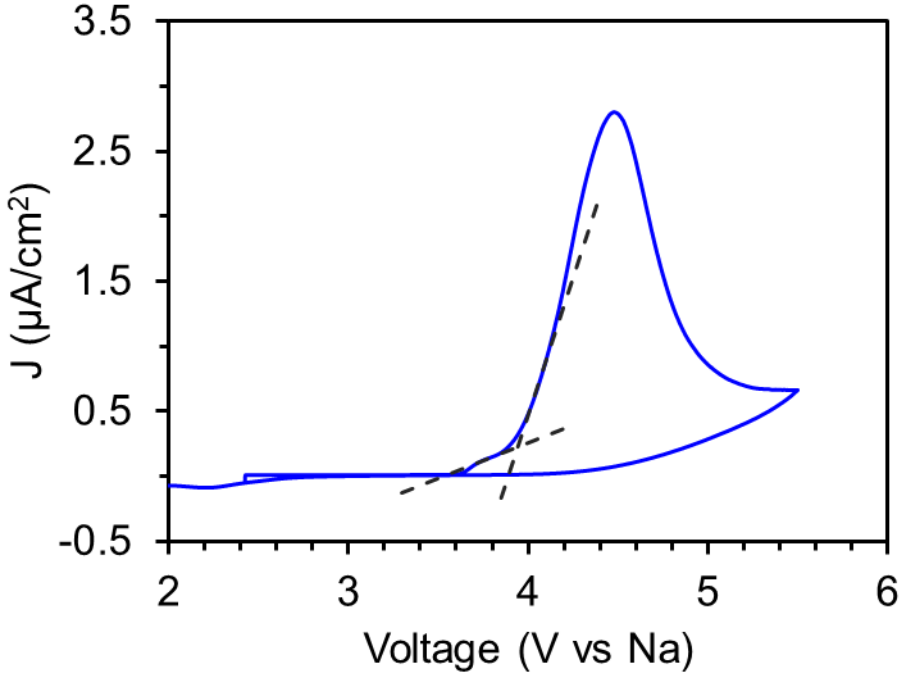

Figure S12. Cyclic voltammetry curve of $NaCB_9H_{10}$ in Li/SE/SE-SS/SS (SS=stainless steel) at a scan rate of 0.1 mV/s at 25°C.

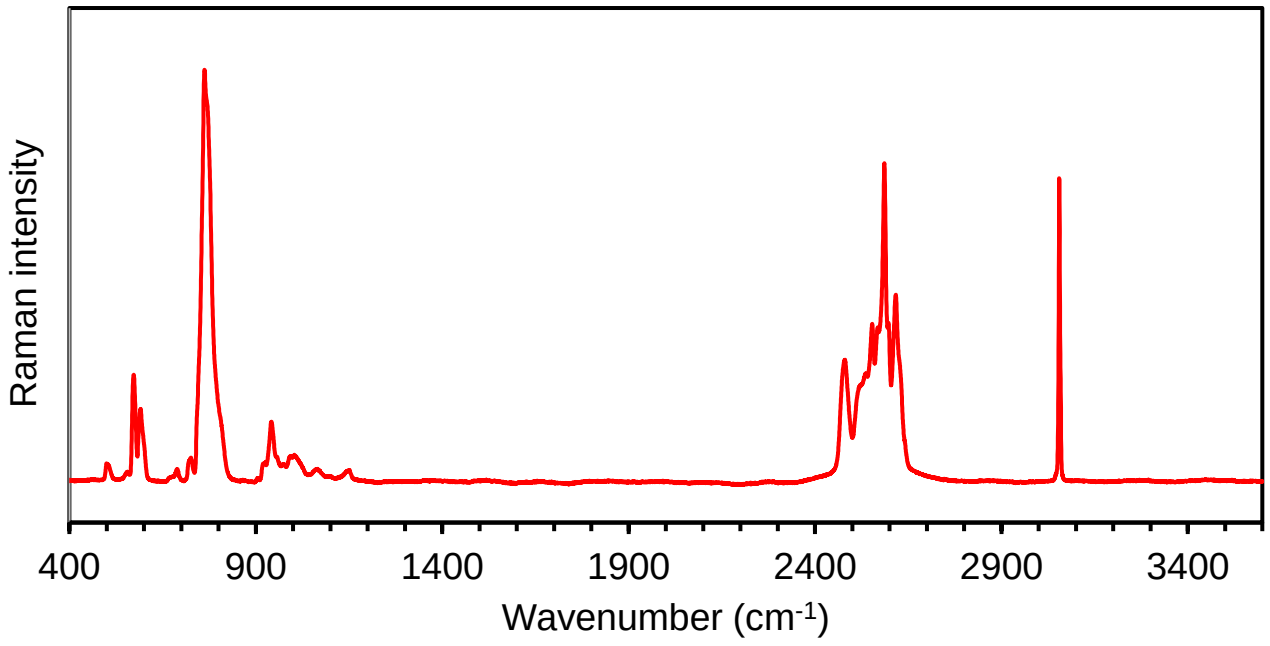

Figure S13. Raman spectrum of $LiCB_{11}H_{12}$.

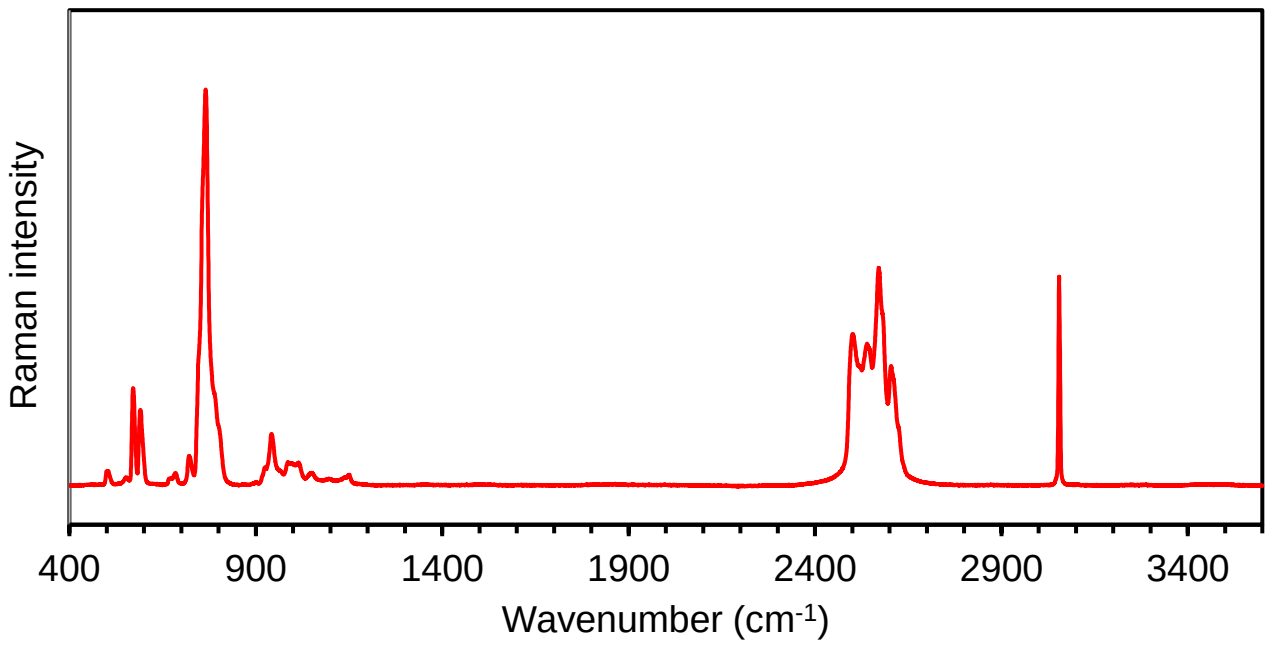

Figure S14. Raman spectrum of $NaCB_{11}H_{12}$.

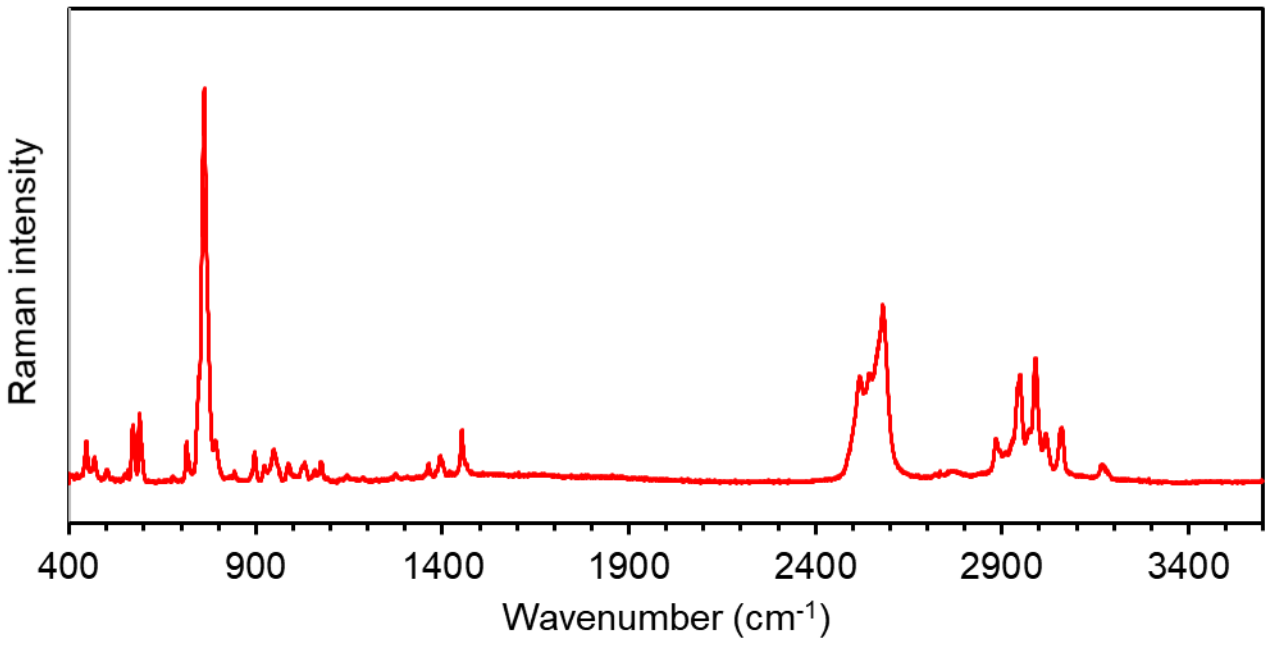

Figure S15. Raman spectrum of $HNEt_3CB_{11}H_{12}$.

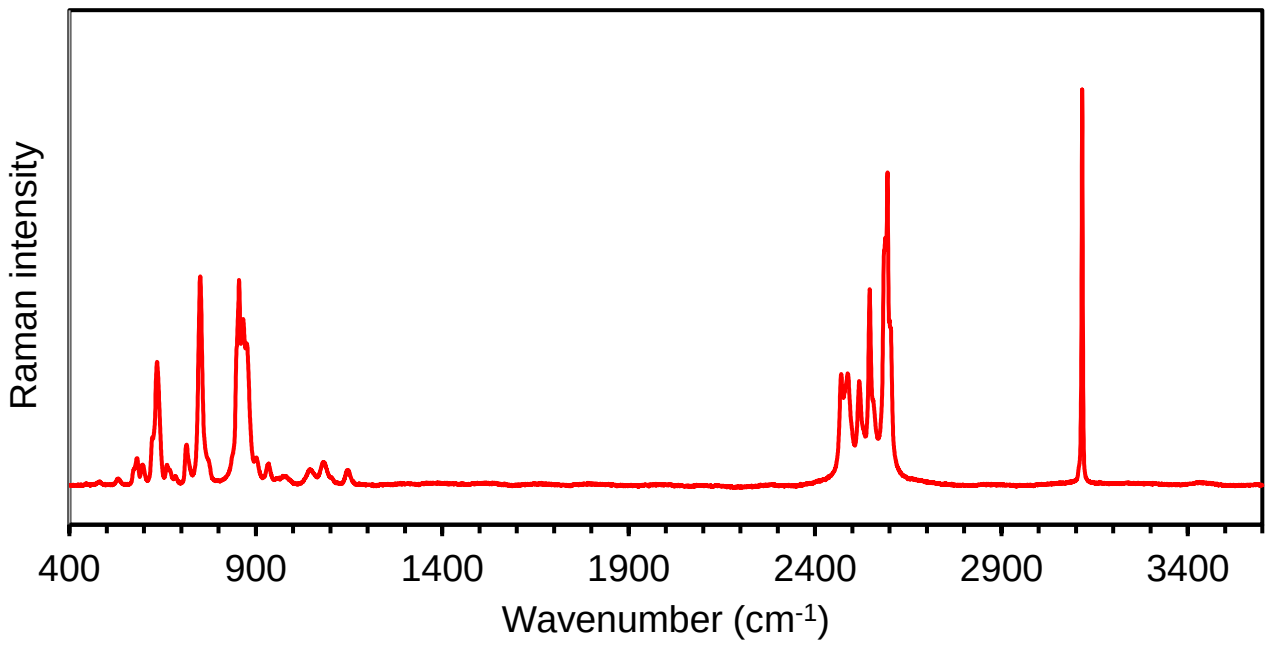

Figure S16. Raman spectrum of $LiCB_9H_{10}$.

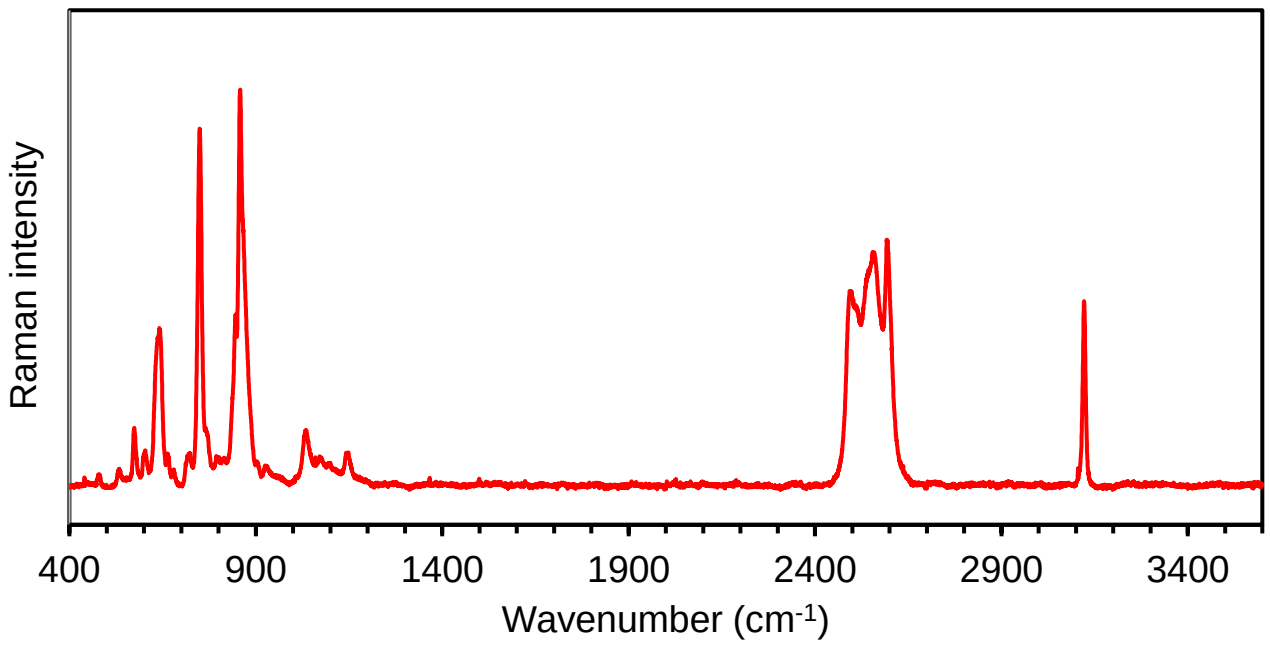

Figure S17. Raman spectrum of $NaCB_9H_{10}$.

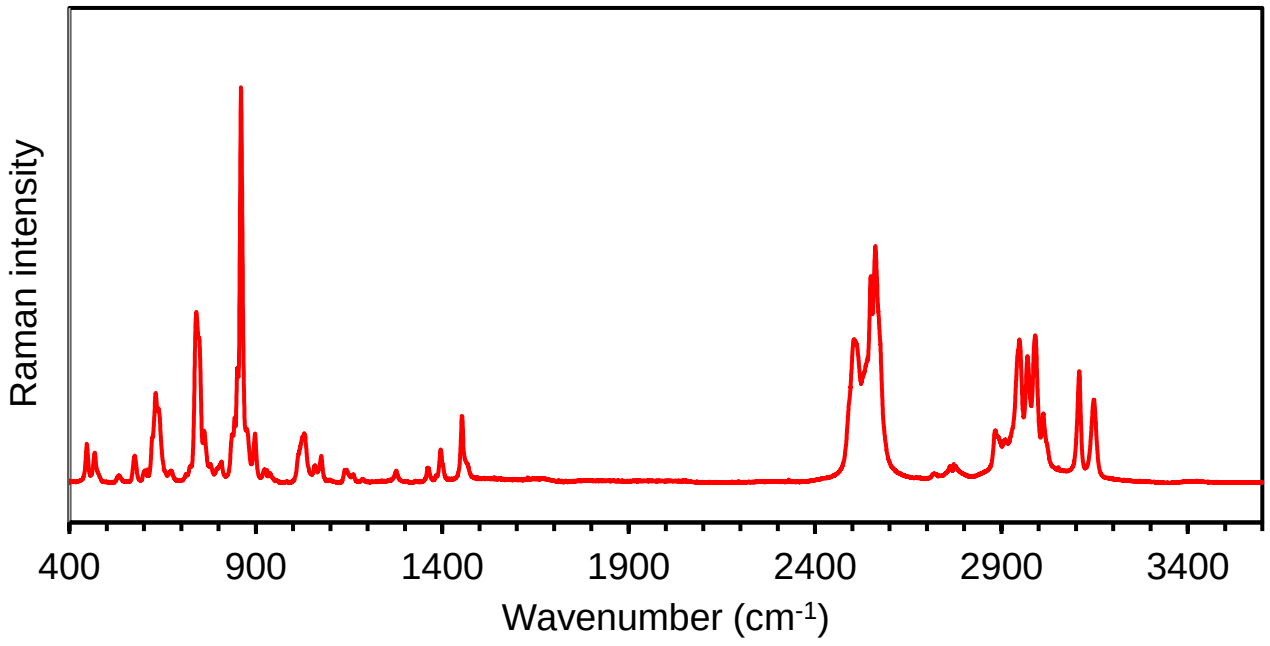

Figure S18. Raman spectrum of $HNEt_3CB_9H_{10}$.

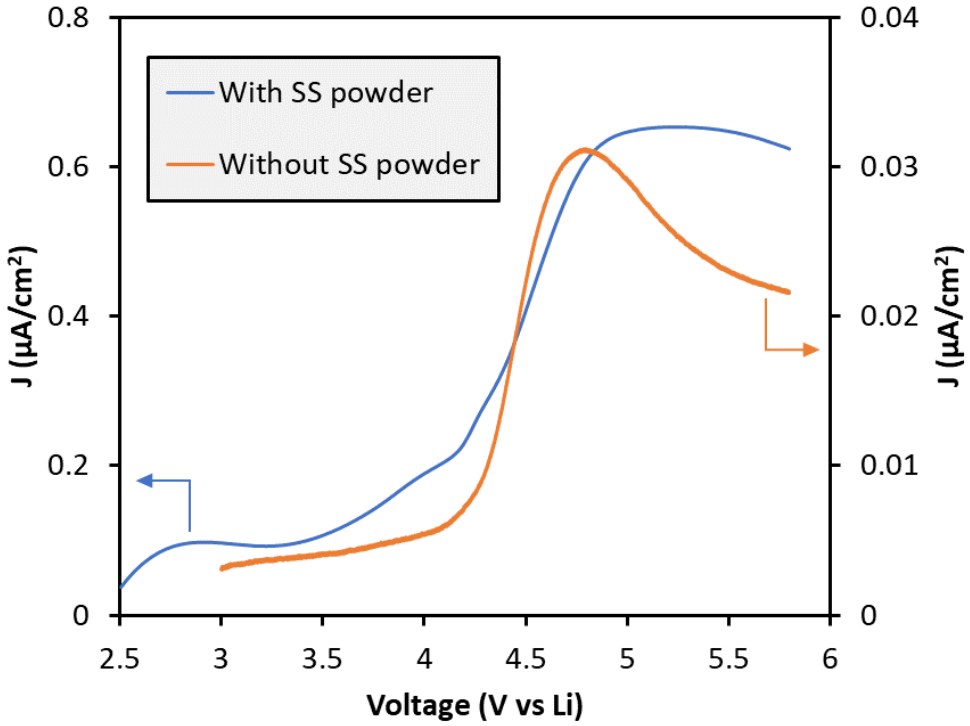

Figure S19. Anodic linear scan voltammograms of $LiCB_{11}H_{12}$ in Li/SE/SE-SS/SS (SS=stainless steel; SE/SS ratio is 1:1 by volume) and Li/SE/SS cells at a scan rate of 0.1 mV/s at 25°C.

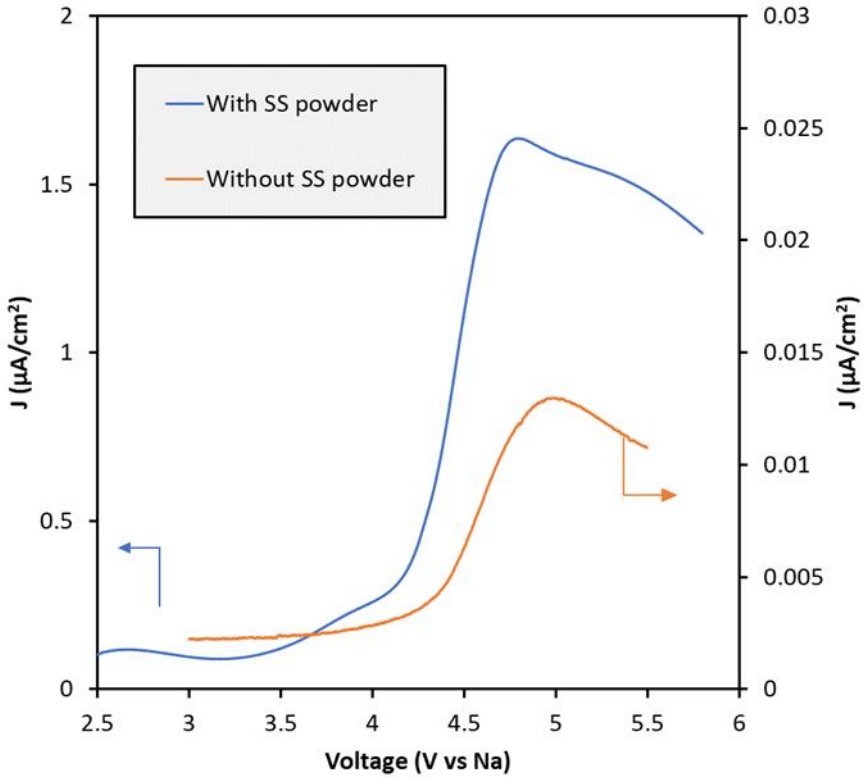

Figure S20. Anodic linear scan voltammograms of $NaCB_{11}H_{12}$ in Na/SE/SE-SS/SS (SS=stainless steel; SE/SS ratio is 1:1 by volume) and Na/SE/SS cells at a scan rate of 0.1 mV/s at 25°C.

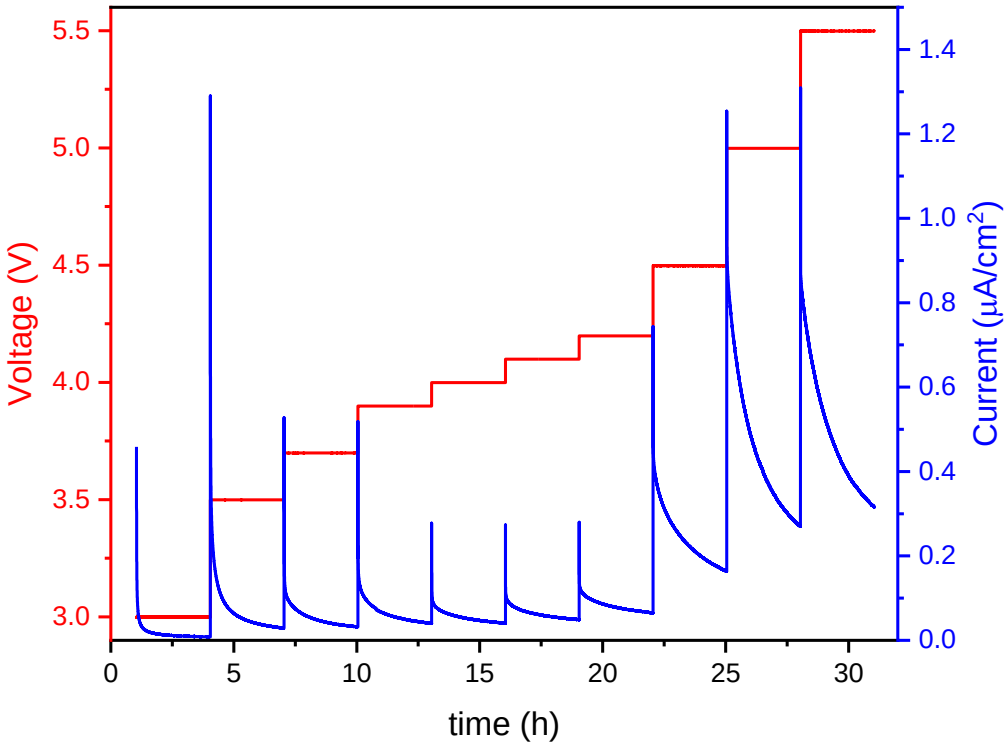

Figure S21. DC polarization curves of $LiCB_{11}H_{12}$ in a Li/SE/SS-SE/SS (SS=stainless steel; SE/SS ratio is 1:1 by volume) between 3-5.5 V vs Li.

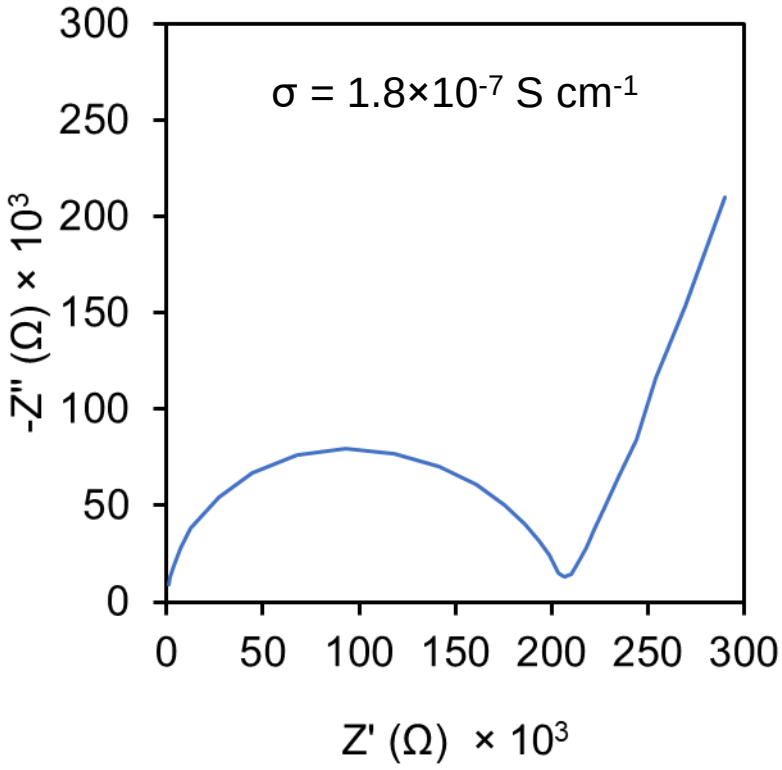

Figure S22. Impedance plot of a SS/$LiCB_{11}H_{12}$/SS cell (SS=stainless steel) at 30°C. Electrode surface area=0.94 cm^2, pellet thickness=357 μm.

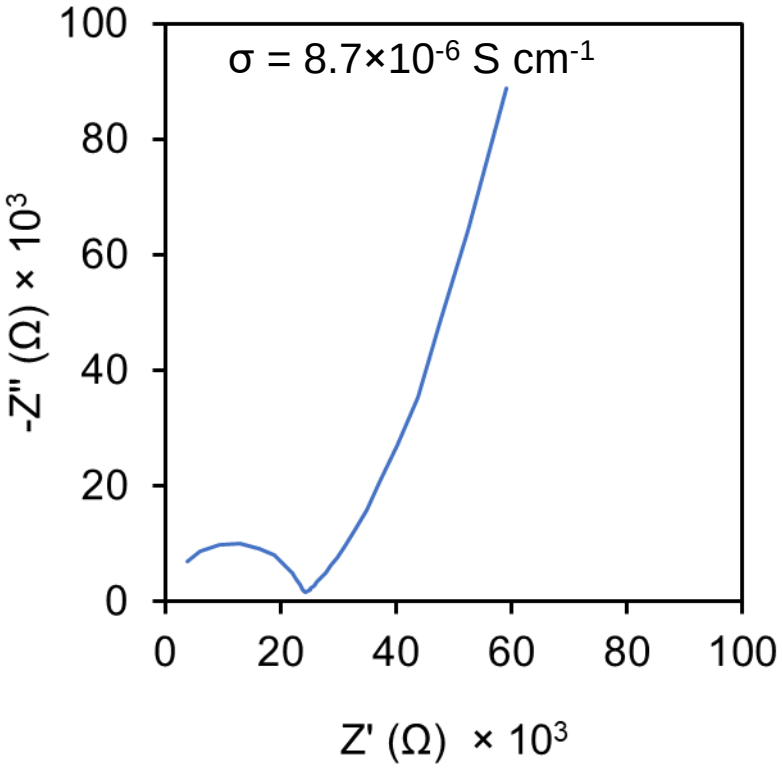

Figure S23. Impedance plot of a SS/$NaCB_{11}H_{12}$/SS cell (SS=stainless steel) at 30°C. Electrode surface area=0.94 cm^2, pellet thickness= 210 µm.

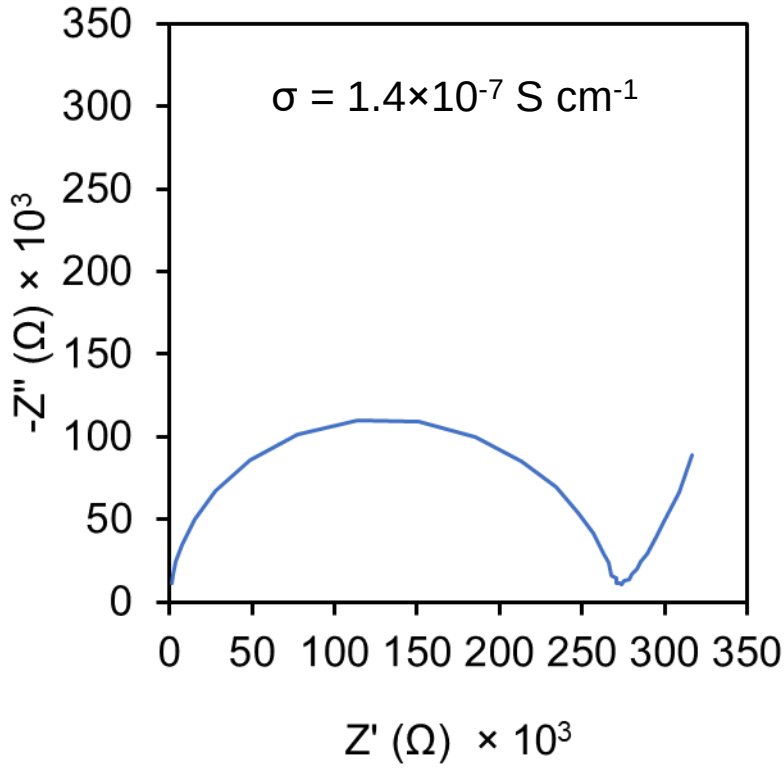

Figure S24. Impedance plot of a SS/$LiCB_9H_{10}$/SS cell (SS=stainless steel) at 30°C. Electrode surface area=0.94 cm^2, pellet thickness=368 µm.

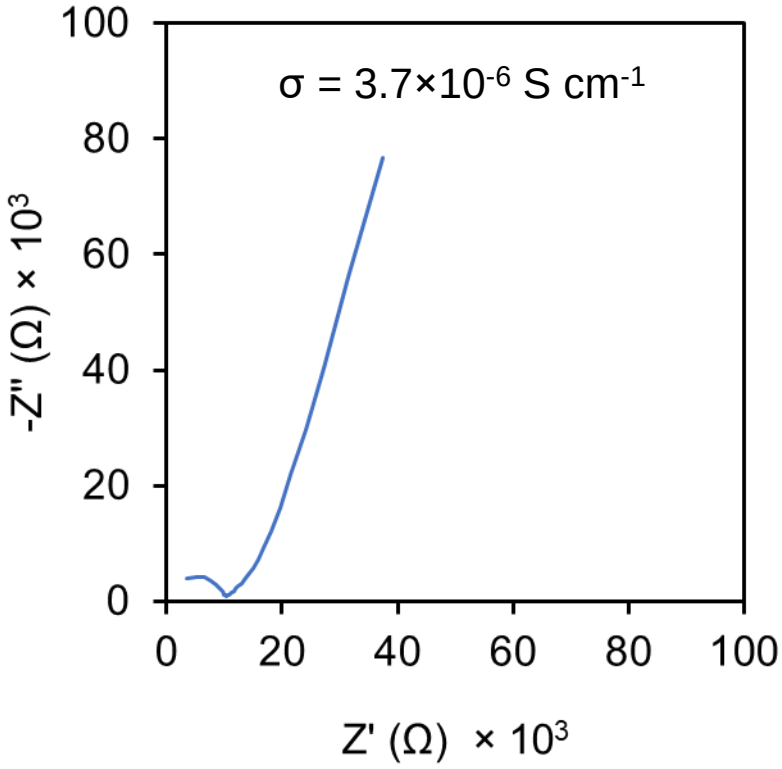

Figure S25. Impedance plot of a SS/$NaCB_9H_{10}$/SS cell (SS=stainless steel) at 30°C. Electrode surface area=0.94 cm^2, pellet thickness=444 µm.